Properties of Working Electrodes with Diamond Blends in Dye Sensitized Solar Cells

Minkyoung Choi, Yunyoung Noh, and Ohsung Song[†]

Department of Materials Science and Engineering, University of Seoul, Seoul 02504, Korea

(Received May 26, 2015; Accepted July 2, 2015)

ABSTRACT

We prepared blocking layers by adding 0.0 ~ 0.6 wt% nano diamond blends (DBs) to TiO_2 blocking layers to improve the energy conversion efficiencies (ECEs) of dye sensitized solar cells (DSSCs). TEM and micro-Raman spectroscopy were used to characterize the microstructure and phases of DBs, respectively. Optical microscopy and FE-SEM were used to analyze the microstructure of the TiO_2 blocking layer with DBs. UV-VIS-NIR spectroscopy was used to determine the absorbance of the working electrodes. A solar simulator and a potentiostat were used to determine the photovoltaic properties and the impedance of the DSSCs with DBs. From the results of the DBs analysis, we determined a 6.97 nm combination of nano diamonds and graphite. We confirmed that ECE increased from 5.64 to 6.48 % when the added DBs increased from 0.0 to 0.2 wt%. This indicates that the effective surface area and electron mobility increased when DBs were added to the TiO_2 blocking layer. Our results indicate that the ECE of DSSCs can be enhanced by adding an appropriate amount of DBs to the TiO_2 blocking layers.

Key words : Diamond blend, Spin coating, Blocking layer, Energy conversion efficiency, Dye sensitized solar cell

1. Introduction

Dye sensitized solar cell (DSSC) is a type of solar cells being operated by the similar principle to that of photosynthesis, and is composed of a working electrode part which generates electrons and positive holes and moves electrons upon, a counter electrode part which receives light delivering electrons to an electrolyte through an external circuit, and an electrolyte for oxidation and reduction actions.[1] Also, since production costs of the DSSC are reasonable compared with currently commercialized silicon solar cells and production of devices of diversified colors and control of transparency allowed, it may be applied to a variety of areas such as building windows and automobile glasses, etc.[2]

However, there is a problem in the case of the DSSC where somewhat low efficiencies around 12% have been observed thus far whereas energy conversion efficiencies of 25% are exhibited by silicon solar cells.[3] To improve such low efficiencies of the DSSC, studies are being conducted actively on engineering of individual components such as counter electrode part, dye part, working electrode part, etc. For the counter electrode, studies on increasing the efficiencies by making double layer structures of Cr/Pt, etc. in the place of Pt employed as a catalyst in the past have been reported,[4] while studies have been published on enabling

an increase in the efficiencies through expansion of the wavelength band of absorbable light by adding phosphor materials to the dye part.[5]

For efficiency improvement studies through engineering of the working electrode part, much investigation is being conducted for addition of new materials capable of increasing specific surface areas and electron mobilities of the working electrode part. In the case of engineering to increase specific surface areas of the working electrode part, structure improvement of TiO_2 layer or blocking layer is being realized, and X. Luan *et al.*[6] have reported that specific areas of the working electrode as well as efficiencies are increased when TiO_2 layer is produced to have a structure of nano rod, nano tube. In the case of engineering to increase electron mobilities of the working electrode part, Dubacheva *et al.*[7] improved electron mobilities by adding to the TiO_2 layer carbon allotropes such as C_{60}, carbon nanotube, graphene, etc., while Zhang *et al.*[8] reported that efficiencies were improved from 3.63% to 6.34% by improving electron mobilities through addition of CNT to TiO_2. However, studies on a simultaneous increase in both specific surface areas and electron mobilities are scarce.

Diamond blend (DB) is unrefined nano diamond (ND) including various impurities which are produced first upon ND generation by explosion method. Therefore, there is an advantage of being economical in comparison with commercially refined ND. While it is produced as carbon atoms instantaneously form SP_3 bonding under a high-temperature, and high-pressure environment, atomic bonding fails to be completely changed at this time and other carbon allotropes such as carbon nanotube, graphene, carbon black,

---

[†]Corresponding author : Ohsung Song
 E-mail : songos@uos.ac.kr
 Tel : +82-2-6490-2410   Fax : +82-2-6490-2404

etc. having SP_2 bonding come to exist as impurities. Each carbon allotrope has a different band gap structure as in graphene (0 eV), carbon nanotube (1.71 eV), graphite (1.72 eV), and diamond(5.5 eV). Other allotropes excluding diamond have a structure consisting of SP_2 bonding, and are characterized by a high thermal conductivity and a small band gap compared with TiO_2 (3.2 eV) along with an excellent electron mobility due to a lower energy level of conduction band.[8] When the DB having such characteristics was applied to the DSSC, an improvement in electron mobilities is expected by reduction of a difference in energy levels among dye, TiO_2, FTO substrate through carbon allotropes together and an improvement in specific surface areas due to ND by using characteristics of nano-class particles.

In the present study, possibility of efficiency improvement in the DSSC through improvements in specific surface areas and electron mobilities was affirmed while 0.00, 0.02, 0.05, 0.20, 0.30, 0.50, 0.60 wt% of DB were added to the blocking layer.

2. Experimental Procedure

In the present study, 0.0 ~ 0.6 wt% of diamond (Korea Technology Trade Co., Ltd.) was prepared for evaluation of properties resulting from addition of diamond blend (DB) to the blocking layer of a dye sensitized solar cell (DSSC) device. The DB employed here was a product having a particle size of 6 ~ 10 nm, and ND purity of 50%.

To check for microstructures of the DB, an analysis was conducted by using TEM (Transmission electron microscope, JEOL Co., JEM-2100F). After drying following drop on the upper part of a grid coated with carbon film subsequent to dispersion of the DB mixed with ethanol using ultrasonic waves, it was mounted on a TEM instrument holder for observation of magnified images.

Also, DB compositions were checked by using a micro-Raman spectrograph (UniThink Co., UniRaman). Here, the specimen was placed on a silicon wafer with a high reflectivity after dispersing DB in ethanol, and characteristic peaks of main component carbon allotropes were checked with the noise removed by scanning for 60 times in an accumulation mode where the exposure value for light source was 5 seconds, at a center value of 2000 cm^{-1} in a range of 1100 ~ 2800 cm^{-1}.

For production of a blocking layer for the working electrode, blocking layers of various conditions were produced by spin coating under the conditions of 500 rpm for 10 sec., 2000 rpm for 40 sec. following dispersion of 7 types of the mixed solutions with addition of 0.00, 0.02, 0.05, 0.20, 0.30, 0.50, 0.60 wt% of DB, respectively, to a mixed solution of titanium (IV) bis (ethyl aceto acetato)-diisopropoxide and 1-Butanol by using an ultra sonicator.

In addition, to check for microstructures of the blocking layer, surfaces were observed under an optical microscope (Carl Zeiss Co., Scope. A1), while surfaces of the blocking layer were observed in FE-SEM (field emission scanning electron microscope, Hitachi Co., S-4800) by using an acceleration voltage of 15 kV.

TiO_2 film was prepared by coating of TiO_2 paste (Dyesol DSL 18NR-T of 10) having a particle size of 20 nm on the produced blocking layer using doctor blade method followed by heat treatment at 500°C for 30 minutes. Subsequently, a working electrode having a structure of glass/FTO/blocking layer (TiO_2 with diamond blends)/TiO_2/dye (N719) was finally completed by adsorbing 0.5 mM cis-vis bis-ruthenium (II) bis-tetrabutylammonium (N719).

To check for absorbance of the produced working electrode resulting from DB addition, an analysis was conducted by using UV-VIS-NIR (Shimadzu Co., UV3105PC). Here, absorbance measurements for each sample were completed by mounting an instrument for absorption mode and setting the scan speed at a medium value. To find an average absorbance in the visible light bandwidth in the range of 400 ~ 800 nm, an average value was obtained by adding absorbances at each wavelength band and dividing the sum by the frequency of addition.

For production of a counter electrode, 100 nm Pt was vapor-deposited across the entire face of a flat glass substrate by using a RF sputter (MHS-1500, Moohan. Co., 300 W, 13.56 MHz). As a target for Pt thin film deposition, 99.99% Pt was used, respectively, while 40 sccm Ar was used as a reaction gas at room temperature (RT) under a process pressure of 5 mtorr for production of a thin film.

The DSSC device of 0.45 cm^2 in effective area having a vertical cross section of glass/FTO/blocking layer (TiO_2 with diamond blends)/TiO_2/dye (N719)/electrolyte/100 nm Pt/glass was finally completed by joining the prepared working electrode part and the counter electrode part and by inserting an electrolyte.

To check for opto-electrical characteristics of the DSSC device, I-V (current-voltage) was measured by using a solar simulator (PEC-L11, Peccell) and a potentiostat (Iviumstat, Ivium). At this time, an analysis was made by using a light source of 100 W Xenon lamp under the condition of 1 sun (100 mW/cm^2). For the I-V analysis, short circuit current density, open circuit voltage, fill factor, and energy conversion efficiency were checked together. To check for an interfacial resistance of the completed device, impedance measurements were also conducted.

3. Results and Discussion

Figure 1 is a TEM image taken for the microstructure of DB. Size of a DB particle was measured to be 6.98 nm, and the structure was agglomeration of several particles having a sphere form due to strong agglomeration forces between carbon allotropes.[9] In view showing of particles is a sphere one, carbon nanotube having a crystalline structure of tube shape is not considered to exist, and carbon allotropes included as impurities in the DB were presumed to be graphite or graphene having a sphere form.

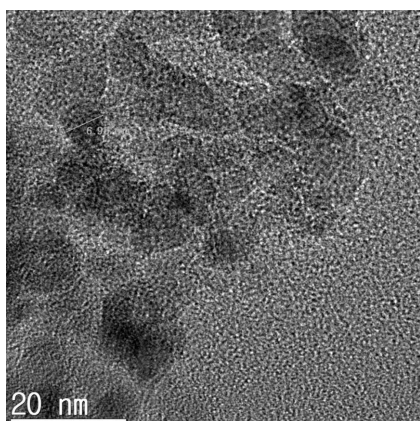Figure 2 represents a Raman result for the analysis of
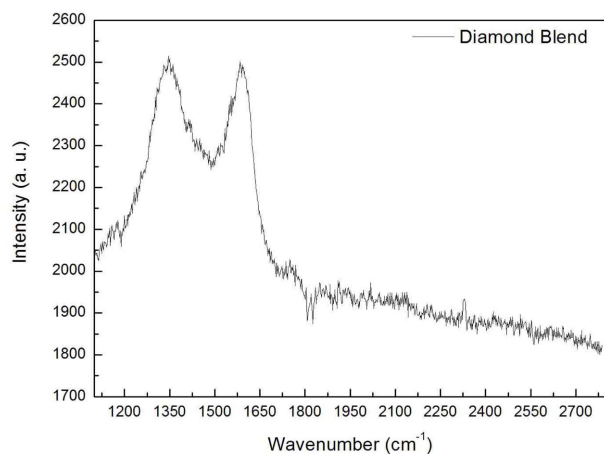
Fig. 1. TEM image of the nano diamond blend.

Fig. 2. Raman spectrum of the diamond blend.

Fig. 3. Optical images of the blocking layer with (a) 0.0 wt% DB, and (b) 0.5 wt% DBs. Insets are magnified from FE-SEM images.

Fig. 4. UV-VIS-NIR spectra of the working electrodes with DBs additions.

compositions of carbon allotropes contained in the DB. Two peaks were observed at 1345, 1584 cm^{-1}. The peak at 1345 cm^{-1} was considered to have appeared wide due to overlapping of the characteristic Raman peak of graphite appearing at 1350 cm^{-1} and the Raman peak of diamond appearing at 1332 cm^{-1}. The peak observed at 1584 cm^{-1} was in agreement with the Raman peak of graphite reported by Reich *et al*.[10] Although a peak was observed at 1600 cm^{-1} in the case of graphene in the same way as with graphite, graphene was considered not to exist since no peak appeared at 2700 cm^{-1}.[11] Consequently, according to the Raman analysis results, all impurities contained in the DB employed in the present study were considered to be present in the form of graphite.

Figure 3 is an optical microscope image observed at 500 times magnification for a device coated onto a FTO substrate by spin coating method after dispersing 0, 0.5 wt% of DB in the blocking layer. The figure inserted at the top on the right side is a FESEM of the same device analyzed at 25000 times magnification. In the case of the blocking layer with addition of 0.0 wt% DB in (a), uniform coating of the blocking layer along the irregularities of FTO layer could be affirmed, and in the case of addition of 0.5 wt% DB in (b) as compared with this, uniform distribution of the shapes of
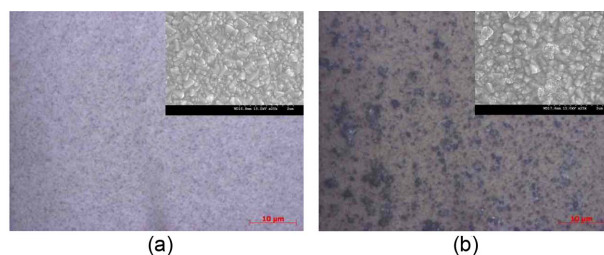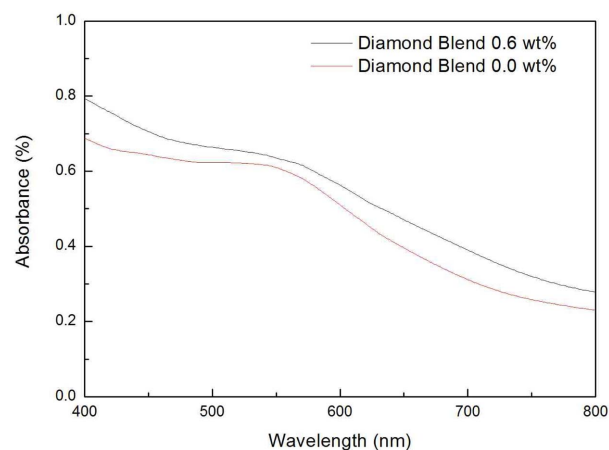
black agglomerates throughout surfaces could be affirmed so that successful realization of DB dispersion was ascertained as intended.

Shown in Fig. 4 is an absorbance graph of the working electrode part measured by UV-VIS-NIR. When amounts of DB addition were 0.0, 0.6 wt%, average values of absorbance in the wavelength band of 400 ~ 800 nm were shown to be 0.48, 0.53, respectively. As compared with the case of no addition, absorbance could be affirmed to increase in the case of DB addition, which is a result that specific surface areas of the blocking layer were increased due to DB addition and hence adsorption amounts of dye were increased accordingly.

Figure 5 shows a Nyquist diagram consisting of real numbers and imaginary numbers for the frequencies imposed on a DSSC device of glass/FTO/blocking layer (TiO$_2$ with DBs)/TiO$_2$/dye (N719)/electrolyte/100 nm Pt/glass structure with DBs additions of 0.0 ~ 0.6 wt%. As with internal resistance of a general DSSC, 3 types of semi-circles (R$_1$, R$_2$, R$_3$) were affirmed to appear. R$_1$ value is related to the resistance of FTO/TiO$_2$ interface and the resistance of electrolyte/counter electrode interface to movement of electric charges at 10^3-10^5 Hz, showing similar values of about 1.6 Ω upon addition of 0.0 ~ 0.6 wt% of DB.

Also, R$_2$ value is related to the resistance to movement of electric charges in TiO$_2$ at 1-10^3 Hz, and it could be seen to
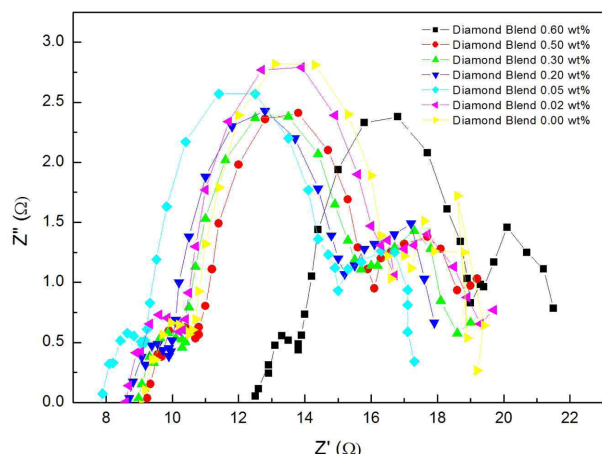
Fig. 5. Impedance spectra of the DSSCs with DBs additions.

Table 1. Photovoltaic Performance and Energy Conversion Efficiency of DSSCs with DBs Additions

DB contents (%)	Open circuit voltage (Voc)	Fill factor (FF)	Short circuit current density (Jsc)	Energy conversion efficiency (η)
0.00 wt%	0.66	0.65	13.10	5.64
0.02 wt%	0.67	0.65	13.28	5.75
0.05 wt%	0.66	0.65	14.52	6.19
0.20 wt%	0.66	0.63	15.58	6.48
0.30 wt%	0.65	0.63	15.85	6.44
0.50 wt%	0.65	0.63	15.06	6.11
0.60 wt%	0.66	0.61	15.12	6.05

decrease to 6.5, 5.9, 5.3, 5.4, 5.4, 5.2 Ω, respectively, in the case of a device with DB addition while a value of 6.1 Ω was shown for the device with 0 wt% addition. This was considered to be attributable to an increase in electron mobilities due to an effect of graphite with a smaller band gap compared with TiO_2 resulting from addition of DB to TiO_2. In the meanwhile, Warburg impedance R_3 related to oxidation-reduction reaction of the electrolyte showed a similar value of about 2.7 Ω due to the use of the same electrolyte.

Therefore, the resistance to electric charge movement in TiO_2 could be affirmed to decrease as an effect of graphite with a small band gap upon addition of DB to the blocking layer.

Table 1 shows I-V data of a DSSC device resulting from DB addition, indicating the results for open circuit voltage, fill factor, short-circuit current density and energy conversion efficiency.

In the case of open-circuit voltage (Voc), similar values were shown at about 0.66 V within an error range, since the same electrolyte was used as a factor affecting oxidation-reduction reaction of the electrolyte.

In the case of fill factor (FF), similar values were shown within an error range, since the same TiO_2 paste and Pt electrode as well as electrolyte were used as a factor affecting interfacial resistance.

In the meanwhile, in the case of short-circuit current density (Jsc), it may be affirmed to increase and then decrease with the amounts of DB addition, which meant that resistance to electron movement could be reduced and changes in band gap could occur to reduce recombination of electrons as an effect of graphite with a smaller band gap compared with TiO_2 among the impurities contained in the DB. Such changes in band gap were considered to play the role of reducing a loss of electrons as electrons produced from the dye move from the semiconductor oxide layer to the blocking layer, which showed a result in agreement with the reduction in R_2 values indicative of resistance to electron movement as shown previously in the impedance results. When

DB addition is excessive being higher than 0.3 wt%, the short-circuit current density can be seen to rather decrease, which was considered to be a result of reduction in movement paths of electrons due to a relative reduction in the fraction of TiO_2 layer as an electron transmission material with an increase in amounts of DB addition.

In the case of energy conversion efficiency (η), it was changed in a similar way to the short-circuit current density since open-circuit voltage and fill factor were measured to be almost similar as a result of DB increase. Namely, while it was gradually increased with addition of DB to the blocking layer so that an efficiency of 6.48% was observed upon addition of 0.2 wt% DB in comparison with an efficiency of 5.64% observed upon addition of 0.0 wt% DB, showing a maximum efficiency increase by 1.15 times. Such increase in the efficiencies could be explained as being attributable to a decrease in the resistance to electron movement by DB addition as with the short-circuit current density and to the corresponding increase in the short-circuit current density.

4. Conclusions

To improve efficiencies of dye sensitized solar cells (DSSCs), 0.0 ~ 0.6 wt% of diamond blend (DB) was added to the blocking layer and the corresponding changes in material properties and opto-electrical characteristics of the DSSC were affirmed. With addition of DB to the blocking layer, resistances to electron movement were decreased while efficiencies of the device were increased. Final efficiencies of the final device were increased upon DB addition up to 0.2 wt%, which resulted from an increase in electron mobilities as a material with a small band gap was added. In the meanwhile, efficiencies were decreased when the amounts of DB addition were more than 0.3 wt%, and this is attributed to a decrease in the short-circuit current density due to a reduction in the areas of electron transmission path as a result of a relative decrease in the fraction of TiO_2 with an increase in the amounts of DB addition. Consequently, efficiencies of a DSSC device could be increased by adding an appropriate amount of DB to the blocking layer.

Acknowledgments

REFERENCES

1. B. O' Regan and M. Gratzel, "A Low-cost, High-efficiency Solar Cell Based on Dye-sensitized Colloidal TiO$_2$ Films," *Nature*, **353** 737-40 (1991).

2. K. Wongcharee, V. Meeyoo, and S. Chavadej, "Dye-sensitized Solar Cell Using Natural Dyes Extracted from Rosella and Blue Pea Flowers," *Sol. Energy Mater. Sol. Cells*, **91** 566-71 (2007).

3. M. A. Green, K. Emery, Y. Hishikawa, W. Warta, and E. D. Dunlop, "Solar Cell Efficiency Tables," *Prog. Photovolt: Res. Appl,* **22** 701-10 (2014).

4. Y. Noh and O. Song, "Properties of the Cu/Pt Bilayered Counter Electrode Employed Dye Sensitized Solar Cells," *Korean J. Met. Mater,* **52** 557-60 (2014).

5. S. Bai, C. Wang, H. Fatima, C. Bu, S. You, Z. Yu, N. Cheng, H. Hu, S. Guo, and X. Zhao, "A Novel Glowing Electrolyte Based on Perylene Accompany with Spectrum Compensation Function for Efficient Dye Sensitized Solar Cells," *J. of Power Sources*, **280** 430-34 (2015).

6. X. Luan, L. Chen, J. Zhang, G. Zu, J. C. Flake, and Y. Wang, "Electrophoretic Deposition of Reduced Graphene Oxide Nanosheets on TiO$_2$ Nanotube Arrays for Dye-sensitized Solar Cells," *Electrochimica Acta*, **111** 216-22 (2013).

7. G. V. Dubacheva, C. K. Liang, and D. M. Bassani, "Functional Monolayers from Carbon Nanostructures – Fullerenes, Carbon Nanotubes, and Graphene – as Novel Materials for Solar Energy Conversion," *Coord. Chem. Rev.,* **256** 2628 (2012).

8. S. Zhang, H. Niu, Y. Lan, C. Cheng, J. Xu, and X. Wang, "Synthesis of TiO$_2$ Nano Particles on Plasma-treated Carbon Nanotubes and Its Application in Photoanodes of Dye-Sensitized Solar Cells," *J. Phys. Chem.*, **115** 22025-34 (2011).

9. S.Iijima, M. Yudasaka, R. Yamada, S. Bandow, K. Suenaga, F. Kokai, and K. Takahashi, "Nano-aggregates of Single-walled Graphitic Carbon Nano-horns," *Chem. Phys. Lett.*, **309** 165-70 (1999).

10. S. Reich and C. Thomsen, "Raman Spectroscopy of Graphite," *Phil. Trans. R. Soc. Lond*, **362** 2271-88 (2004).

11. D. Yoon, H. Moon, H. Cheong, J. S. Choi, J. A. Choi, and B. H. Park, "Variations in the Raman Spectrum as a Function of the Number of Graphene Layers," *J. Korean Phys. Soc.,* **55** 1299-303 (2009).